

# Sequential recruitment and combinatorial assembling of multiprotein complexes in transcriptional activation

Vincent Lemaire,<sup>1,\*</sup> Chiu Fan Lee,<sup>2,\*</sup> Jinzhi Lei,<sup>3,1</sup>  
Raphaël Métivier,<sup>4</sup> and Leon Glass<sup>1</sup>

<sup>1</sup>Centre for Nonlinear Dynamics, McGill University, Canada

<sup>2</sup>Physics Department, Clarendon Laboratory  
Oxford University, UK

<sup>3</sup>Zhou Pei-Yuan Center for Applied Mathematics  
Tsinghua University, China

<sup>4</sup>UMR 6026, Équipe EMR, Université de Rennes 1, France

February 5, 2008

## Abstract

In human cells, estrogenic signals induce cyclical association and dissociation of specific proteins with the DNA in order to activate transcription of estrogen-responsive genes. These oscillations can be modeled by assuming a large number of sequential reactions represented by linear kinetics with random kinetic rates. Application of the model to experimental data predicts robust binding sequences in which proteins associate with the DNA at several different phases of the oscillation. Our methods circumvent the need to derive detailed kinetic graphs, and are applicable to other oscillatory biological processes involving a large number of sequential steps.

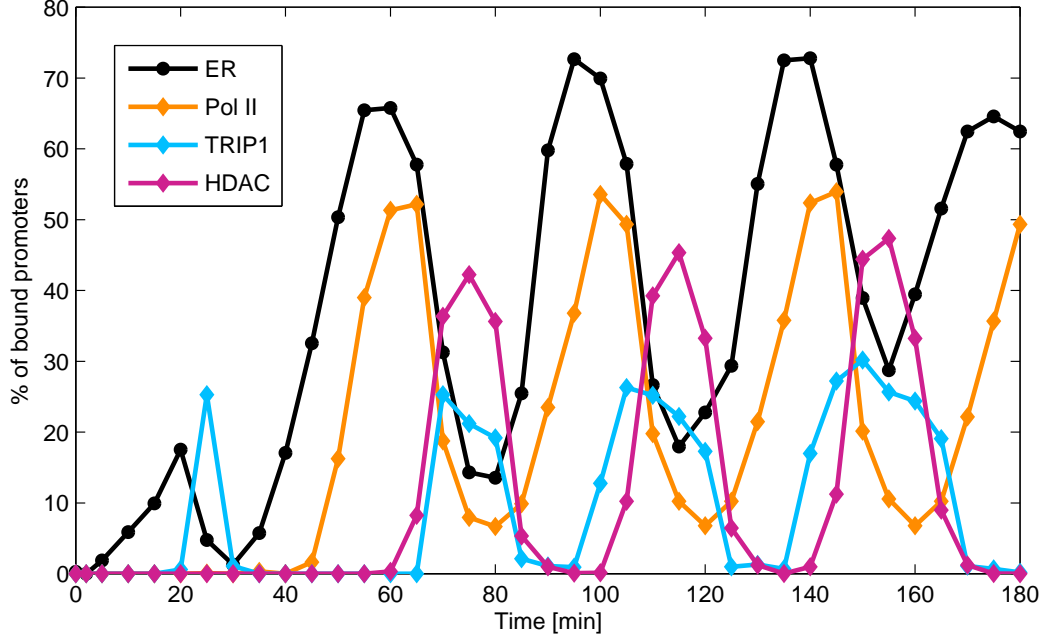
The central dogma of molecular biology states that for a given gene, the sequence of nucleotide bases in DNA is transcribed into messenger RNA which in turn is translated into a specific sequence of amino acids that constitute the protein coded by the initial gene. In higher organisms, such as ourselves, transcriptional control is a crucial step in the regulation of gene expression. This control is modulated by the configuration of proteins around

promoters (DNA regions in the proximity of genes that carry out the integration of transcriptional signals). Although there are a large number of theoretical models of transcriptional control networks [1] and transcriptional control of a single gene in prokaryotes [2], theoretical analysis of transcriptional control of a single gene in eukaryotes is much less developed [3].

Histones and other protein molecules associate with the DNA to form chromatin, the constituent of the chromosomes of eukaryotes. In order for transcription to occur, chromatin must be unfolded from its condensed geometry in which DNA is compactly wrapped around the histones. Although full details are still not well understood, it is clear that sequential chemical reactions between the histone molecules and specialized enzymes underlie the modification of the chromatin structure [4]. For example, acetylation of the histones leads to a more open chromatin configuration, by changing the local electrostatic equilibrium of the molecular ensemble around where the modification is made, enabling transcription [5]. On each histone protein there are a number of different amino acids sites at which chemical reactions can occur leading to a modification of the histone–DNA geometry. The histone code hypothesis posits that the modifications of the histones provide a code which governs the subsequent chemical processes leading to the remodeling of the chromatin [6].

Recent experimental studies have demonstrated a cyclic ordered sequence of reactions and alterations of local chromatin structure in human breast cancer cells grown in tissue culture [7]. The culture of approximately  $2 \times 10^6$  cells is initially synchronized. The addition of a hormone, estradiol, induces 40 min oscillations of the transcriptional activation of the pS2 gene, which is a marker gene for estrogenic response. Due to loss of synchronization between the cells, the observed oscillations slowly damp and reach constant levels after 8 hours [8]. A possible source of desynchronization, in addition to stochastic fluctuations at the level of the promoter, could be the variability among the cells, such as ATP levels or cell size. These oscillations are monitored by measuring the temporal association of specific proteins with the DNA measured at time intervals of as short as 5 minutes over a 3 hour period [9]. In Fig. 1, we show the association profiles of four key proteins involved in the transcriptional activation of gene pS2. Estrogen receptor (ER) binds estradiol and initiates the transcription process. RNA Polymerase II, (Pol II) is a protein complex responsible for the transcription of genes. TRIP1 and HDAC are two different proteins that are involved in the clearance of the promoter after each transcription cycle. In view of the complexity of the sequence, and the tiny numbers of molecules involved in the binding in each cell, it is currently impossible to derive detailed kinetic data about the rate constants of the individual reactions. Moreover, since it is not clear whether

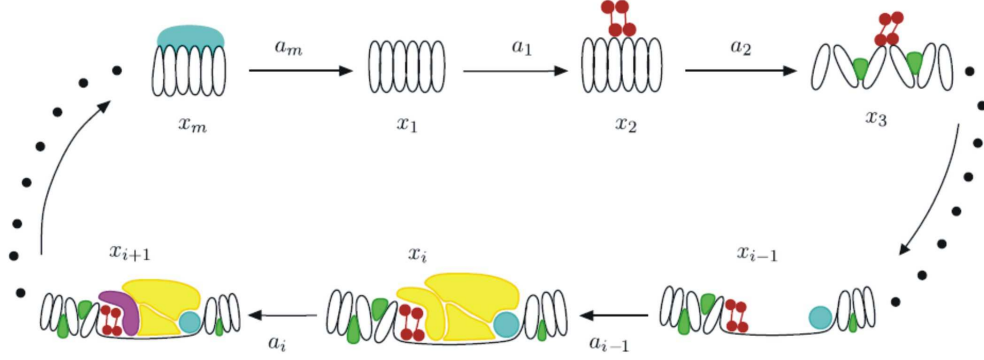
Figure 1: (color online). Dynamics of proteins binding at the pS2 promoter following administration of estradiol in MCF-7 human breast cancer cells. The proportions of bound pS2 promoters with key transcription factors and cofactors are shown as a function of time. Based on data from Ref. [7].



or not the cells are coupled to each other, the mechanism of the synchronization of the oscillation poses a challenge for theoretical interpretation. In this Letter, we propose a simple model for the oscillation based on a large number of sequential chemical reactions and transformations of the chromatin. Based on the analysis of the model, we are able to predict specific timings of the association of the protein complexes with the chromatin that reproduces the observed dynamics in Fig. 1.

We assume that there is a network of proteins interacting together and, sequentially, with the chromatin. Each reaction induces a modification of the substrate complex that in turn enables the next step in the sequence so that the reactions are assumed to be irreversible. Further, we assume that the various transcription factors and cofactors involved in the reactions are present in sufficiently high concentration that the reaction rates  $a_i$  are constant over time. This model is schematized in Fig. 2. A key parameter in our model is the number  $m$  of sequential steps in the cycle. Many transcription complexes contain more than 50 proteins, which may be partially or completely assembled on the promoter [10]. Of the order of 100 histone (or

Figure 2: (color online). A schematic diagram of the model by sequential recruitment of protein molecules to the chromatin.  $x_1$  represents the chromatin at the pS2 promoter. The  $x_i$ ,  $2 \leq i \leq m$  represent the protein complexes that form successively on the promoter, at rate  $a_i$ , leading to the activation of transcription.

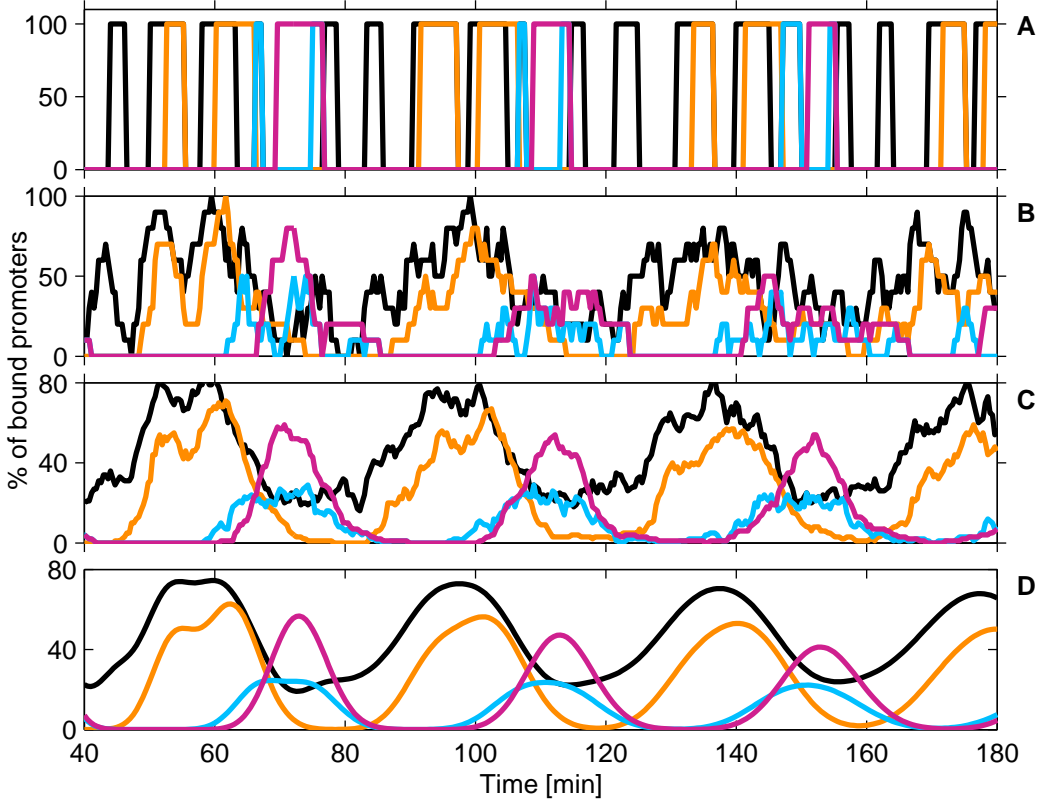


other proteins) modifications have been identified during transcriptional activation [11]. These sequential histone modifications are associated with the histone code for transcriptional activation. Based on these considerations, we estimate that  $m$  is at least 200. From the data in Fig. 1, the period of the oscillation  $T_0$  is about 40 minutes. If all reaction rates are assumed identical (i.e.,  $a_i = a$ ), and choosing  $m = 200$ , then we have  $a = m/T_0 = 5\text{min}^{-1}$ .

Since, generally, there are only two copies of each gene in each cell, we first consider the dynamics using a stochastic model in which the probability of a given reaction per unit time is equal to the product of the rate constant for that reaction and the number of potential reactants present. The time steps between reactions obey a Markov process. The results of carrying out the simulation using the Gillespie algorithm [12], for 1, 10, or 100 cells are shown in Fig. 3A-C.

The chemical scheme presented in Fig. 2 can be interpreted as a sequential Poisson process in which the duration  $t$  before the next reaction takes place follows the distribution  $p(t) = ae^{-at}$ . Then for any individual cell after synchronization, the  $k$ -th cycle has a mean starting time of  $\frac{km}{a}$  with a variance  $\frac{km}{a^2}$ . Taking  $a = m/T_0$ , the starting time of the  $k$ -th cycle has a variance of  $\frac{kT_0^2}{m}$ . This suggests the natural desynchronization of the system as the variance increases linearly with  $k$ . As  $m \rightarrow \infty$ , the variance vanishes and the system behaves as a delay differential system as discussed in Ref. [13]. Thus, just as in the data in Fig. 1, the stochastic system displays oscillations for several cycles provided  $m$  is large enough.

Figure 3: (color online). A-C: Stochastic simulations for 1, 10, or 100 cells. D: Recruitment curves calculated from Eq. (5). These computations are based on the binding sequences given in Fig. 4 (see below). We assume  $a_i = 5\text{min}^{-1}$  and  $m = 200$ . The color (or grayscale) code is the same as in Fig. 1.



In the limit of a large number of cells, the stochastic dynamics can be approximated by the linear differential equations

$$\begin{aligned}\dot{x}_1(t) &= a_m x_m(t) - a_1 x_1(t) , \\ \dot{x}_i(t) &= a_{i-1} x_{i-1}(t) - a_i x_i(t) , \quad 2 \leq i \leq m .\end{aligned}$$

In the case  $a_i = a$ , the eigenvalues  $\lambda_k$  of the Jacobian matrix are  $\lambda_k = a (e^{\frac{2\pi k i}{m}} - 1)$ ,  $1 \leq k \leq m$ . We can rewrite  $\lambda_k$  as  $\alpha_k + i\beta_k$ , where

$$\alpha_k = a (\cos \theta_k - 1), \quad \beta_k = a \sin \theta_k, \quad 1 \leq k \leq m . \quad (1)$$

Here  $\theta_k = 2k\pi/m$ . Since the real parts of the eigenvalues are non-positive, Eqs. (1)-(1) do not show sustained oscillations [14].

Assuming initial conditions, for the  $[x_i]$ , of  $[1, 0, 0, \dots, 0]$ , we can compute the solution for all variables:

$$x_i(t) = \frac{1}{m} \left[ 1 + (-1)^i e^{-2at} + 2 \sum_{k=1}^{m/2-1} e^{\alpha_k t} \cos[\beta_k t - (i-1)\theta_k] \right], \quad (2)$$

in the case when  $m$  is even (a similar expression holds when  $m$  is odd). The higher frequency terms decrease rapidly so that for  $m = 200$ , only the first 6 or 7 terms give a significant contribution after the first period. The leading term  $e^{\alpha_1 t} \cos \beta_1 t$  sets the period. From a Taylor expansion of this result, we find that the envelope of the leading term decays as  $e^{-2\pi^2 t/mT_0}$ , where we set  $a = m/T_0$ . This result is consistent with the finding that the oscillations are more persistent as the number of steps of the reaction increases.

We now consider the effect of relaxing several of the unrealistic assumptions in the model. If all reactions are reversible, with all forward rate coefficients equal to  $a$  and all backward reaction coefficients equal to  $b$ , the real and imaginary parts of the eigenvalues are  $\alpha_k = (a+b)(\cos \frac{2k\pi}{m} - 1)$  and  $\beta_k = (a-b) \sin \frac{2k\pi}{m}$ . This leads to an increased damping, and an increase in the oscillatory period that scales as  $b/a$  for small  $b$  in comparison to  $a$ . Consequently, the main results presented below also hold if the reactions are reversible. A more general discussion on the effects of reversible reactions in chains of linear reaction kinetics is given in Ref. [15].

Since in the biological system, the reaction rates are not identical, we now assume that the forward rates are distributed randomly with probability distribution  $Q(a_i)$ . Realizing that the waiting time for each reaction to occur is independent and identically distributed, the  $k$ -th cycle's starting time has mean and variance,  $km \int \frac{Q(x)}{x} dx$  and  $km \int \frac{Q(x)}{x^2} dx$ , respectively. If, in particular,  $Q(a_i)$  is the uniform distribution over the interval  $[a(1-d), a(1+d)]$ , with  $0 \leq d \leq 1$ , the  $k$ -th cycle's starting time has mean:

$$\frac{km}{2ad} \int_{a(1-d)}^{a(1+d)} \frac{dx}{x} = \frac{km}{2ad} \ln \frac{1+d}{1-d}, \quad (3)$$

and variance:

$$\frac{km}{2ad} \int_{a(1-d)}^{a(1+d)} \frac{dx}{x^2} = \frac{km}{a^2(1-d^2)}. \quad (4)$$

Then the mean and variance of the  $k$ -th period are, respectively,  $\langle T_k \rangle = \langle T \rangle = \frac{m}{2ad} \ln \frac{1+d}{1-d}$  (independent of  $k$ ) and  $\sigma_{T_k}^2 = \frac{(2k-1)m}{a^2(1-d^2)}$ . Thus, on the curve  $\langle T \rangle = T_0$ , we have the variance  $\sigma_{T_k}^2 = \frac{4(2k-1)T_0^2 d^2}{m \ln[(1+d)/(1-d)]^2}$ , which, again, vanishes as  $m \rightarrow \infty$ .

The damping of the solutions of Eqs. (1)-(1) is controlled by the least negative  $\alpha_k$ 's. Let  $a_i = a(1 + \epsilon \omega_i)$  and  $\epsilon = \sigma_a/a$ , where  $\sigma_a$  is the standard

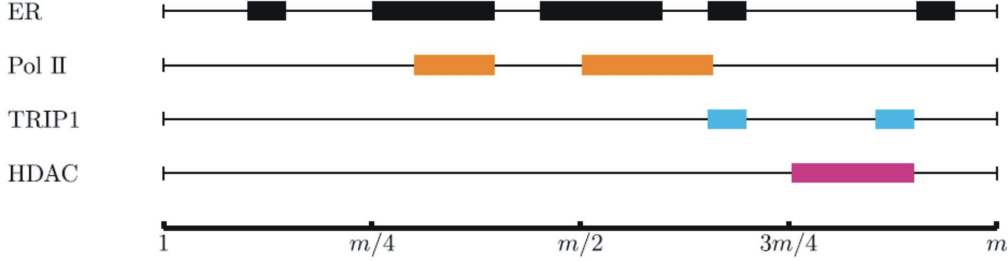
deviation of the  $a_i$ 's. Assuming that  $a_i$  is uniformly distributed in the interval  $[a(1-d), a(1+d)]$ , we have  $\langle a_i \rangle = a$  and  $\sigma_a = ad/\sqrt{3}$ , and then,  $\langle \omega_i \rangle = 0$  and  $\langle \omega_i^2 \rangle = 1$ . Solving the characteristic equation for successive orders in  $\epsilon$ , we find that, to fourth order in  $\epsilon$ ,  $\langle \alpha_k \rangle = a(\cos \theta_k - 1)(1 + o(\epsilon^4))$ , which is consistent with numerical results that show negligible dependence of  $\langle \alpha_k \rangle$  on  $d$ . However, the variance of the  $\alpha_k$ 's is  $\sigma_{\alpha_k}^2 = \frac{\langle \alpha_k \rangle^2}{m} \epsilon^2 + o(\epsilon^4)$ . This shows that the properties of low damping and synchronization of the oscillation, observed when the  $a_i$ 's are identical, are conserved in the limit of large  $m$  when the rate constants are different.

We now wish to fit the model to the experimentally observed binding profiles of the proteins in Fig. 1. Each protein is a component of several different  $x_i(t)$  complexes, but we do not know a priori which ones. We call  $P_j(t)$  the percentage of pS2 promoters bound to one or more molecules of protein  $j$ . Then we have

$$P_j(t) = \sum_{i=1}^m c_{i,j} x_i(t), \quad (5)$$

where  $c_{i,j}$  is either 0 or 1.  $P_j(t)$  is the quantity measured in ChIP experiments shown in Fig. 1. For each protein  $j$ , the *binding sequence*  $\{c_{i,j}\}$  is determined by doing a least squares minimization of the data to the model. Because the first cycle is produced by a different sequence of chemical steps than the subsequent ones [7], we consider only the time points such that  $T_0 \leq t \leq 3T_0$ . The minimization procedure is done in 2 steps: (i) we apply the Nelder-Mead method to minimize the quadratic error, with the constraint that  $0 \leq c_{i,j} \leq 1$  [16]; (ii) we use the values of  $c_{i,j}$  obtained in the first step as initial conditions to a method that uses Lagrange multipliers, minimizing again the mean square error. The latter step enables us to generate binary  $c_{i,j}$ 's. The result of that procedure is shown in the Fig. 4, where the colored regions indicate the regions where  $c_{i,j} = 1$ . The  $P_j(t)$ , for each protein in Fig. 1, are plotted in Fig. 3D. To test the robustness of these fitted sequences, we have carried out a number of numerical studies in which we performed fits of the model to the data relaxing several of our assumptions. In particular, we have tested for values of  $m = 100, 200, 300$  and  $400$ ; addition of  $\pm 2\%$  of noise to the data points (corresponding to the error reported in Ref. [7]); changes in the vertical scaling of the data (up to 1.4); and selection of random reaction rates  $a_i$  (provided that the period, for the selection of  $\{a_i\}$ , is close to  $T_0$ , and the solutions not too damped). Although there can be slight changes in the values of  $i$  where  $c_{i,j} = 1$ , or, in some circumstances, a change in the number of blocks in which  $c_{i,j} = 1$ , the main pattern of the  $c_{i,j}$ 's in Fig. 4 remain unchanged.

Figure 4: (color online). Binding sequences for the proteins in Fig. 1. For each protein, the colored regions indicate the indices  $i$  of the complexes  $x_i$  of which the protein is a component.



The results in Fig. 4, in which the precise patterns of association of each protein are obtained, represent the main predictions of the current work. Although one might have anticipated that there would be a single recruitment block for each protein, the recruitment patterns for proteins considered here may actually occur in two or more blocks. Two experimental methods can be used currently to determine the dynamics of transcription: ChIP assays and fluorescence microscopy-based assays, but these methods seem to produce conflicting results [17]. Our theoretical predictions must be viewed in perspective of these two experimental methods. ChIP assays determine the binding of promoters with specific proteins, but not at the level of one promoter in a single cell. In contrast, fluorescence microscopy assays determine the mobility of proteins around individual promoters, but does not measure binding of individual proteins to one promoter. Using ChIP data, our model enables us to predict successive rounds of protein binding and unbinding. The protein mobility indicated by these multiple binding events, corroborates the observations from fluorescence microscopy assays, reconciling the observations from the two experimental methods. Due to lack of precision at the scale of the isolated promoter, the experimental verification of our findings is currently impossible. However, these results can be correlated with what is known about the biological system. For example, five or six principal complexes, with well-defined functions, are successively formed on the promoter of pS2 [7]. It has been conjectured that the assembling of these complexes is orchestrated by ER at different timings of the cycle [7, 11]. Our finding of five different binding times of ER matches perfectly that conjecture.

To summarize, we have proposed a simple model for the oscillation observed in protein association and dissociation during transcriptional activation in human cells. We have shown that the model produces oscillations with minimal damping for large values of  $m$ . Further, these properties are



conserved when the reaction rates are selected randomly. The current work demonstrates that realistic network architecture models may not be needed in order to unravel the mechanisms of complex reaction sequences at the subcellular level. Our approach relies rather on the finding that synchronous dynamics of protein assembly emerge as a consequence of the large number of intermediate reactions. Our methods should be useful to other systems in which many sequential steps take place but the detailed kinetics are not known. Fitting the model to the data in Fig. 1 resulted in predicted sequences at a time resolution not possible experimentally and, as such, may be invaluable for experimental design and for interpretation of the mechanisms underlying transcriptional activation.

This research has been partially supported by NSERC. We thank Dr. John White and Luz Tavera Mendoza, McGill University for helpful conversations. CFL thanks University College (Oxford) for financial support.

\*The first two authors have contributed equally to the present work.  
Corresponding author: Vincent Lemaire (lemaire@cnd.mcgill.ca)

## References

- [1] H. Bolouri and E. H. Davidson, **Proc. Natl. Acad. Sci. U.S.A.** **100**, 9371 (2003); M. C. Lagomarsino, P. Jona, and B. Bassetti, **Phys. Rev. Lett.** **95**, 158701 (2005).
- [2] N. E. Buchler, U. Gerland, and T. Hwa, **Proc. Natl. Acad. Sci. U.S.A.** **100**, 5136 (2003); J. M. G. Vilar and L. Saiz, **Curr. Opin. Genet. Dev.** **15**, 136 (2005).
- [3] A. Benecke, **Complexus** **1**, 65 (2003); P. Paszek, T. Lipniacki, A. R. Brasier, B. Tian, D. E. Nowak, and M. Kimmel, **J. Theor. Biol.** **233**, 423 (2005).
- [4] W. Fischle, Y. Wang, and C. Allis, **Curr. Opin. Cell Biol.** **15**, 172 (2003).
- [5] J. Sun, Q. Zhang, and T. Schlick, **Proc. Natl. Acad. Sci. U.S.A.** **102**, 8180 (2005).
- [6] T. Jenuwein and C. D. Allis, **Science** **293**, 1074 (2001).
- [7] R. Métivier, G. Penot, M. R. Hubner, G. Reid, H. Brand, M. Kos, and F. Gannon, **Cell** **115**, 751 (2003).
- [8] R. Métivier et al. (unpublished).

- [9] The association is monitored using chromatin immunoprecipitation assay (ChIP) and quantitative polymerase chain reaction (PCR). This allows the isolation and identification of proteins that are bound to a specific region of the DNA.
- [10] R. Roeder, **FEBS Lett.** **579**, 909 (2005); Z. Ma et al., **Mol. Cell. Biol.** **24**, 5496 (2004).
- [11] D. Y. Lee, C. Teyssier, B. D. Strahl, and M. Stallcup, **Endocrine Rev.** **26**, 147 (2005).
- [12] D. T. Gillespie, **J. Phys. Chem.** **81**, 2340 (1977).
- [13] N. MacDonald, *Biological Delay Systems: Linear Stability Theory* (Cambridge University Press, Cambridge, England, 1989); I. R. Epstein, **J. Chem. Phys.** **92**, 1702 (1990).
- [14] J. Z. Hearon, **Bull. Math. Biophys.** **15**, 121 (1953).
- [15] D. Summers and J. M. W. Scott, **Math. Computer Modelling** **10**, 901 (1988).
- [16] J. A. Nelder and R. Mead, **Computer J.** **7**, 308 (1965).
- [17] G. L. Hager, A. K. Nagaich, T. A. Johnson, D. A. Walker, and S. John, **Biochim. Biophys. Acta** **1677**, 46 (2004).